Arch. Metall. Mater. **71** (2026), 2, 637-645

DOI: https://doi.org/10.24425/amm.2026.158856

P. SZOTA[1*], S. MRÓZ[1], A. STEFANIK[1], T. ZYGMUNT[2] M. BOŁDA[2]

FE ANALYSIS OF ROLL WEAR DURING RAILWAY RAIL ROLLING PROCESS

The article presents the development of new roll pass designs for rolling of the MAV48, P50 and 50E2 railway rails under the production conditions of the D-815 rolling mill at ArcelorMittal Poland S.A. The aim of the study was to design, using computer simulations, a roll pass geometry ensuring the required dimensional accuracy of the final product while minimizing roll wear and ensuring stable rolling conditions. The roll pass design was developed using a CAD computer program, which enabled precise modeling of pass geometry and their arrangement in the rolling mill. The developed solutions were verified using numerical simulations, and then implemented in industrial conditions for production. The obtained results confirmed the correctness of the design assumptions and indicated the possibility of implementing the developed roll pass system in industrial practice.

Keywords: Hot rolling process; rolls wear; rail; numerical modelling

1. Introduction

Rolling of railway rails is one of the most demanding processes of plastic forming of steel due to the need to obtain very high geometric accuracy of the profile, appropriate mechanical properties and homogeneous microstructure [1-3]. Rails are a critical element of transport infrastructure, and their quality directly affects the operational safety and durability of tracks [4,5]. However, the rolling process is associated with numerous material, technological, and operational challenges that require precise control of production parameters. Significant problems associated with the rail rolling process can be caused by several factors: the general condition of the feedstock and its uniform heating, improper roll pass shape, and wear on the work rolls. A key issue related to rail rolling is the proper design of the rolls calibration. In the case of the rolling process, there are many widely documented cut-out arrangements [6-8] used both in the initial stage of rail rolling (pre-rolling, elongation and pre-forming of the feedstock) and for the final shaping of the rail. It's crucial to select the appropriate shape of the roll passes for the specific rolling mill.

In the case of rough rolling, it's crucial to ensure proper filling of the roll passes and to avoid overfilling, which can lead to defects in subsequent passes. Due to the relatively simple arrangement of the extension passes, for which it is much easier to select a rolling deformation sequence, the greater problem for this stage of rolling may be the proper guidance of the strand and its introduction into the roll pass (elimination of strand twisting) and maintaining the power reserve [9,10]. More significant problems arise at the next stage of the rolling process, in which the rolled material is divided into parts from which the head and feet are formed. Incorrect design of roll pass during rail rolling may result in: overfilling of the rolling pass in the head zone, and consequently, underfilling in the neck and foot zone and uneven metal flow in the rolling direction, formation of foot creases resulting from overfilling of the roll pass in the foot zone, which results in an increase in the flow rate in the rolls direction. Another problem may also be the asymmetry of the finished rail profile resulting from uneven wear of the rollers, incorrect filling of the roll passes in the head, foot and neck parts (caused by incorrect division of the band on the initial roll passes) [11,12]. Modernization of rail rolling processes is currently being conducted by introducing new product ranges to meet market demands, as well as by modifying the design of the roll pass design to reduce roll wear. That's why, the technological challenge is to obtain finished products that meet dedicated acceptance standards, while reducing the number of work roll regenerations [6,7]. Work rolls used in the hot rolling process must be resistant to cracking and, in terms of sudden kinetic and thermal changes, but mainly to the continuous process of surface

[1] CZESTOCHOWA UNIVERSITY OF TECHNOLOGY, FACULTY OF PRODUCTION ENGINEERING AND MATERIALS TECHNOLOGY, 73 DĄBROWSKIEGO STR., 42-201 CZĘSTOCHOWA, POLAND
[2] ARCELORMITTAL POLAND S.A., POLAND
* Corresponding author: piotr.szota@pcz.pl

degradation resulting from friction and abrasion. Moreover, the wear of the working rolls is increased by the use of deep cuts which are intended to pre-divide the volume of the rolled material (in the rail rolling process, this is the "virtual" division the band into the foot and the head) [11,13]. Currently, many problems related to the roll pass design for shape rolling and rolls wear are eliminated already at the design stage thanks to the use of CAD models and FEM modeling [14-16].

The aim of this study was to develop a roll pass design method for rail rolling rolls in the D-815 rolling mill at ArcelorMittal Poland S.A., taking into account both qualitative and quantitative analysis of roll wear. Qualitative analysis allows for comparative assessment and is not dependent on the amount of material rolled. Quantitative analysis allows for the assessment of roll wear, taking into account the length of the rolled strip. Simultaneous consideration of quantitative and qualitative roll wear allows for a comprehensive assessment of the rolls' operational capabilities during a rolling campaign. Fig. 1 shows the shape and basic dimensions of the rails.

The rails shown in Fig. 1 have a similar mass per linear meter, which for the MAV48 rail is 48.5 kg/m (EN 13674-4), P50 – 51.5 kg/m (GOST R 51685 2022), and 50E2 – 49.9 kg/m (EN 13674-1). MAV48 rails (Fig. 1a) are used mainly on railway lines with medium and heavy traffic on sections with moderate to high train speeds, usually up to 160-200 km/h, on some modernized lines also up to 220 km/h. P50 (Fig. 1b) rails are used mainly on industrial lines, sidings, and shorter track sections. 50E2 rails (Fig. 1c) are used on regional, suburban, and industrial lines, where train speeds are moderate (usually up to 120-160 km/h).

The technical literature describes various variants of the roll pass arrangements used for rail rolling, with their sequence and number depending on the rail dimensions and the required reduction ratio. Typical roll pass design sequences include six to ten roll passes, and for larger profiles this number increases accordingly [8,9]. The number and geometry of the roll passes are dictated by both technological requirements and the constraints of the rolling line configuration, including the arrangement and type of rolling stands, as well as available auxiliary rolling equipment such as sliders and other equipment. At ArcelorMittal Poland S.A., at the Huta Królewska rolling mill, as part of the ongoing research and implementation of rolling technology for MAV48, P50, and 50E2 rails, the MAV48 rails are intended for the Hungarian market, the P50 rails for Eastern Europe, and the 50E2 rails for Western Europe. Due to the implementation of new products on the production line, it was necessary to develop a dedicated roll pass design adapted to the existing rolling mill infrastructure, minimizing roll wear during the rolling campaign.

2. Materials and methods

2.1. The Process of Rolling Railway Rails

The railway rails shown in Fig. 1 are different in the dimensions of individual parts, which include the head, foot and neck. The geometry of these three main elements determines the geometry at the initial stage of rolling. From the perspective of developing roll pass design, the cross-sectional areas of individual rail elements are crucial, due to their different dimensions, as is the case for the implemented range. The MAV48 rail is characterized by a large head, a narrow neck, and a narrow foot. The P50 rail has the highest height with a small head and medium neck and foot widths. The 50E2 rail has a medium head but a wide foot measuring 140 mm, which is the largest dimension for this rail weight. TABLE 1 shows the characteristic surface areas of the rails. The data presented in TABLE 1 show that railway rails have different ratios of the head, foot, and neck areas to the total cross-sectional area. This necessitates the use of different pass geometries from the very beginning of the rolling process. Therefore, it is not possible to develop a generalized roll pass design for the analyzed type of rails.

Based on data regarding the technological conditions of the D-815 ArcelorMittal Poland S.A. rolling mill, a roll pass

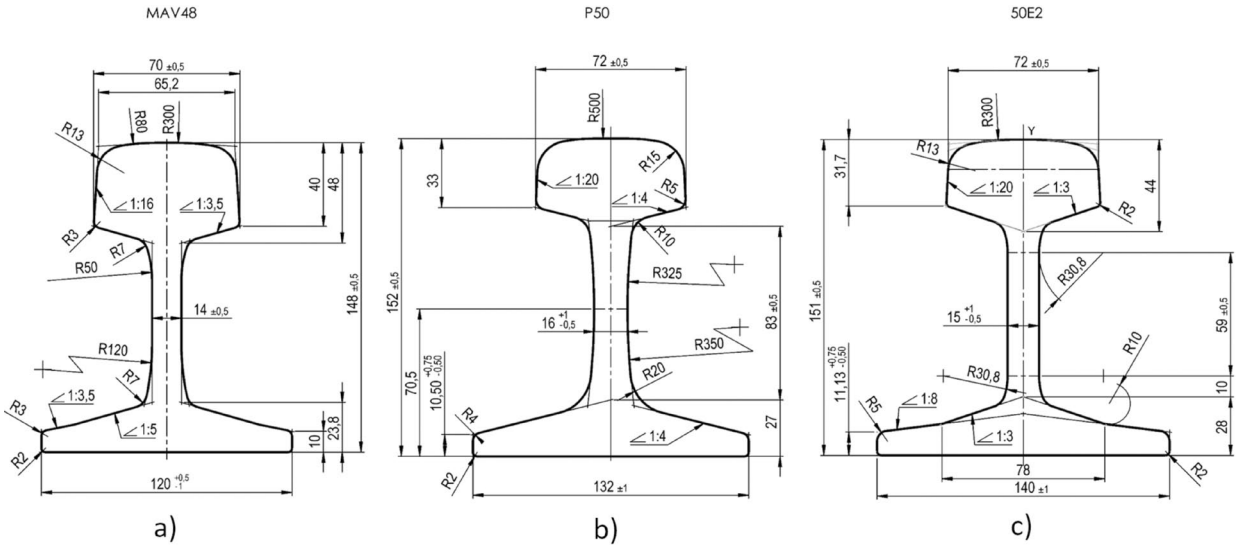

Fig. 1. Shape and dimensions of the rail cross-section: a) MAV48 [17], b) P50 [18], c) 50E2 [19]

TABLE 1

Cross-sectional areas of individual rail elements

Rail type	Mass [kg/m]	Area [mm²]				Percentage share [%]		
		head	foot	neck	total	head	foot	neck
MAV48	48.50	2904.2	2058.0	1216.5	6178.7	47.00	33.31	19.69
P50	51.50	2486.8	2456.2	1654.0	6596.9	37.70	37.23	25.07
50E2	49.90	2584.4	2440.9	1340.0	6365.2	40.60	38.35	21.05

system was developed for three rails: MAV48, P50, 50E2. The rolling pass configuration for all rails was the same, consisting of 10 passes (Fig. 2), which can be divided into pre-forming passes, foot and head forming passes, and finishing passes. The first four passes are responsible for creating the initial shape and thickness of the rail foot by dividing the feedstock into two parts and widening them.

In passes I-III, double-sided notches were used, which facilitate a more favorable distribution of strains in the rolled material, especially in its central part. This solution improves the rail properties and reduces the risk of cracking of the foot in the finished product. In pass 4, a so-called "inverted hat" material is rolled, the shape of which determines the correct division of the rolled feedstock into the head and foot in pass 5 (Fig. 2). In pass 4, the ratio of the feedstock width to the width of the central, thicker part of the strand is important. Equally important is the ratio of the height of the side parts of the strand to the central height of the strand. The preformed feedstock is then directed to pass 5, which is responsible for the correct division of the material into the rail head and foot parts. Proper metal distribution at this stage of the rolling process is one of the key steps in the rolling process to ensure obtaining the appropriate finished product. In the next two passes, 6 and 7, the cross-section is reduced, the rail neck width is increased, and the thickness is reduced. The rail foot is lengthened by alternating closed and open groove rolling with simultaneous thickness reduction. In the last passes, 8-10, the final rail geometry is formed. During rail head forming, to achieve the required corner radii, the metal is deliberately pushed towards the roll. This technique involves alternating changes in the head and foot height relative to the rail axis, forcing the metal to flow towards the foot arms and enabling a larger width compared to previously rolled profiles. A distinctive feature of the designed roll pass system is the shape of the passes in passes 6-10, equipped with diagonally arranged locks that alternate in subsequent passes. This solution enables precise shaping of the thickness and width of the head and foot. Additionally, passes 6-10 are tilted at a specific angle relative to the horizontal axis of the rolls, eliminating the risk of the feedstock jamming in the pass during rolling. The developed roll pass design requires preliminary verification, which was conducted using numerical modeling (FEM).

2.2. Numerical Modeling of the Railway Rail Rolling Process

To conduct computer simulations of the rolling process, it was necessary to develop computer models of the working rolls and the rolled feedstock. Based on the developed models, a simulation project was prepared, which took into account the temperature distribution across the cross-section of the rolled band. Cooling was simulated between successive passes, taking into account the increasing time between passes resulting from the lengthening of the feedstock after each pass. In the case of steel rolling, the deformation state, which depends on the temperature distribution and the strain rate, had to be taken into account [20]. Due to the significant influence of temperature on the plastic flow and stress, the temperature distributions were transferred to the subsequent passes of the numerical modelling rolling process.

The Forge NxT 2.1 computer program was used for the numerical calculations [21]. The theoretical studies of the viscoplastic model of the deformed material for modelling the rolling

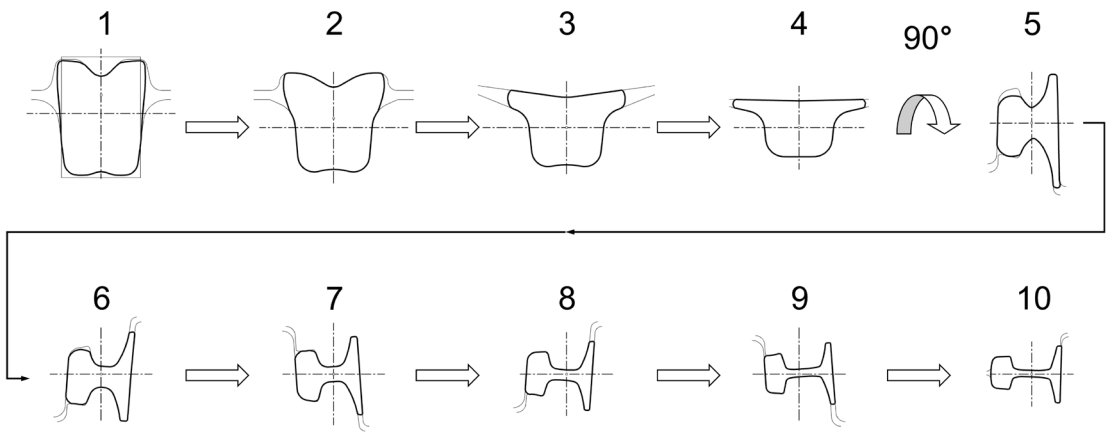

Fig. 2. General layout of the roll pass design used for rolling the analyzed rail types

process of railway rails, the Norton-Hoff law is implemented in this model to describe the mechanical state of the deformed material [22,23].

The flow curves of the R260 steel used in the study were adopted based on plastometric studies conducted at the Częstochowa University of Technology using the Gleeble 3800-GTC physical-thermal simulation system from Dynamic Systems Inc. [12]. Based on the results of the plastometric tests performed in the true strain range from 0 to 1.2, for four strain rates values: 0.1 s^{-1}, 1 s^{-1}, 10 s^{-1} and 100 s^{-1} at temperatures of 900°C, 1000°C, 1100°C and 1200°C, the flow curves of the deformed material were determined [12]. Example plastic metal flow curves are shown in Fig. 3.

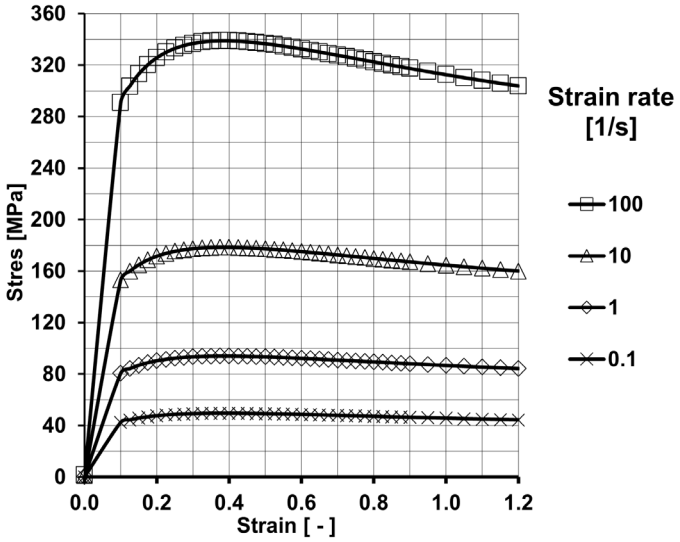

Fig. 3. Plastic flow curve of R260 steel grade obtained during Gleeble 3800 at 900°C

In order to correctly model the rail rolling process, the following material parameter values were assumed: friction coefficients $\mu = 0.4$ (Coulomb); $m = 0.8$ (Tresca) [10,12,21]; ambient temperature – 293K; Poisson's ratio – 0.33; rolling speed 3 m/s, heat capacity = 0.48 kJ/(kg K), density = 7850 kg/m^3, conductivity = 29.9 W/(m K), heat transfer coefficient 10 kW/(m^2 K) [12].

The numerical calculations performed allowed for checking the correctness of the roll passes filling and for analysing the state of deformation and stress as well as the force and energy parameters.

The specified rolling process conditions and parameters allowed for the calculation of the friction work, which is a component of the Archard model defining abrasive wear.

The wear model is described by the following general Eq. (1) [24,25]:

$$WEAR = k_w \int_0^t \frac{\sigma_n v_s}{H(T)} dt, \text{ mm} \tag{1}$$

where: k_w – wear coefficient, v_s – tangential slip velocity of the metal on the tool surface, t – time, $H(T)$ – hardness of the tool at a specific temperature.

In the model described by Eq. (1), it is assumed that under abrasive wear conditions, the volume of material removed from a unit of tool surface is directly proportional to the normal stress σ_n acting on the tool surface and the sliding velocity v_s, and inversely proportional to the hardness $H(T)$ of the material being worn (tool hardness at the specified temperature). Using the assumed initial values, the distribution of *UWFF* values on the model surface can be calculated using formula (2):

$$UWFF = \int_0^t \sigma_n \cdot v_s dt, \text{ mm MPa} \tag{2}$$

3. Results of the numerical modeling

The results of the numerical calculations, apart from verifying the correctness of the developed roll pass design, also allowed for the quantitative assessment of the wear of the rolls for subsequent rolling passes. In the Forge NxT 2.1 wear model, assumes that under abrasive wear conditions, the volume of material V separated from a unit tool surface is directly proportional to the normal stress σ_n acting on the tool surface and the sliding velocity v_s, and inversely proportional to the hardness of the material H undergoing wear (in this case, the temperature-dependent tool hardness). The distribution of the unit friction work *UWFF* (2) is shown for the subsequent cuts in Fig. 4. A qualitative assessment of roll wear can be made based on the distribution of the unit friction work values which are shown in Fig. 4. Higher *UWFF* values quantitatively indicate areas where roll wear will be greatest. As part of the study, the areas with the greatest wear were marked in red and blue on the roll. Red marks the central areas of the rolls, while blue marks the side areas. For these areas with the highest unit friction work values, an analysis was performed for all rolls for three rail types: 50E2, MAV48, and P50. Three *UWFF* measurements were taken in each area and then averaged. These areas are the most important for roll wear, as they most often require reconditioning or resurfacing by regenerating the roll surface. A summary of the averaged measurement results is shown in TABLE 2 (where: **M**iddle – measurement of the middle part of the groove, **S**ide – measurement in the side part of the groove, **UR** – upper roll, **LR** – lower roll) for both the upper and lower rolls. The results in the table are graphically presented in Fig. 5.

Based on the data shown in Fig. 5, it can be concluded that during railway rail rolling, the side surfaces of the groove undergo significant wear in the first phase of rolling, as shown in Fig. 5b. Increased values of the specific friction force work on the side surfaces and in the bottoms of the groove occur for the first four passes, this is particularly true for the lower grooves of the roll passes. Fig. 5a shows the specific friction force work values in the central part of the groove, with the highest values occurring for the upper roll, particularly in the first two passes. Comparing the unit values of friction force work, it can be concluded that for the lower roll, these values are even several times

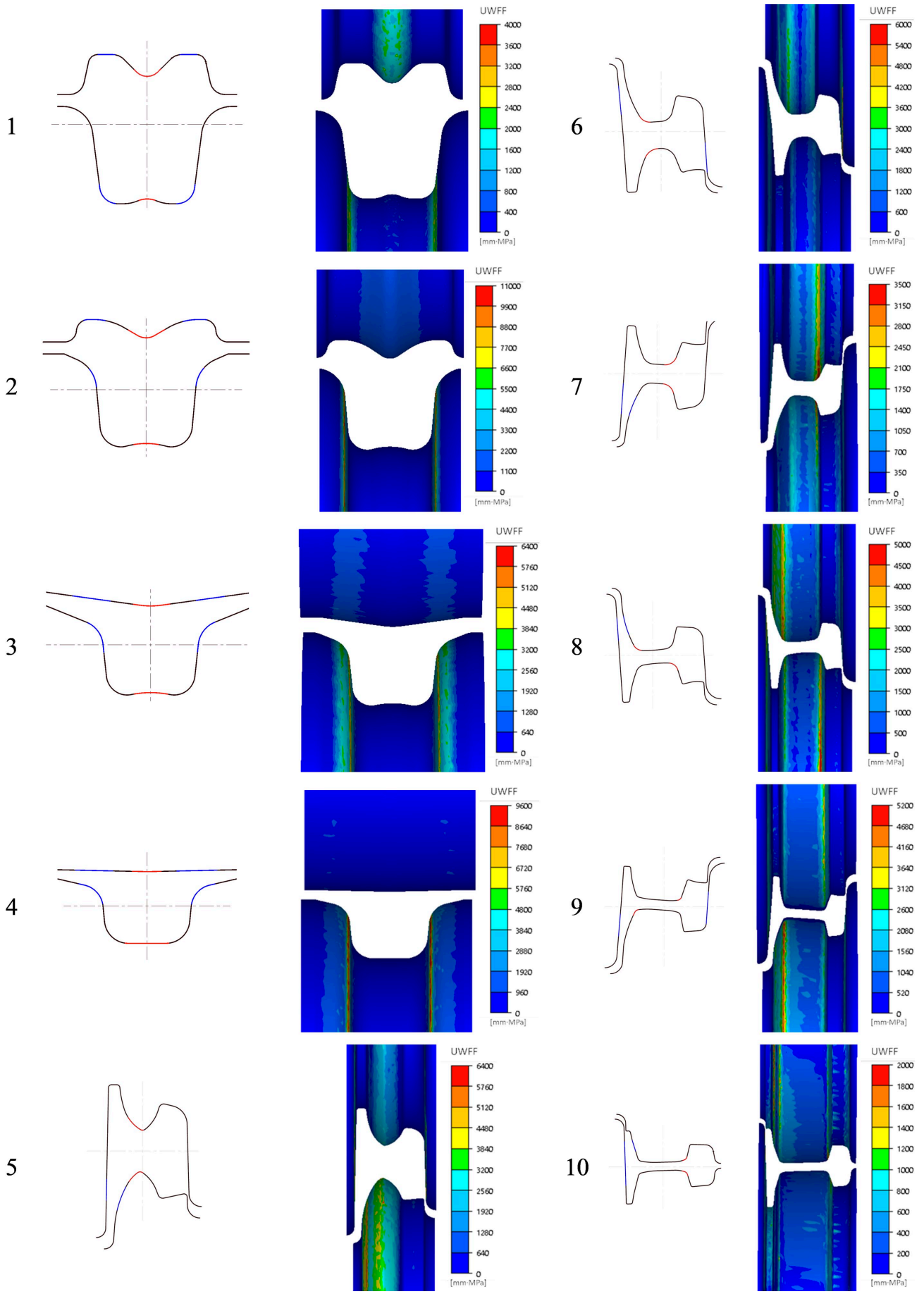

Fig. 4. Measurement points of the roll wear on the cross-section and the unit value of the friction force *UWFF* for the 50E2 rail on the surface of the upper and lower roll in subsequent passes

TABLE 2

Measurement results of the unit work of friction forces for three types of rails

Pass	Unit Work of Friction Force – *UWFF*, [mm·MPa]											
	50E2 UR		50E2 LR		MAV48 UR		MAV48 LR		P50 UR		P50 LR	
	M	S	M	S	M	S	M	S	M	S	M	S
1	1679.0	0.0	359.7	2720.3	1604.3	0.0	240.0	4555.0	1956.7	0.0	373.0	6086.3
2	1630.7	0.0	110.7	9255.7	1255.0	969.3	101.0	15465.0	1002.3	238.0	89.0	10809.7
3	55.7	731.0	233.0	4927.3	341.7	1308.3	294.0	7523.3	289.7	992.3	167.3	7499.0
4	202.0	733.0	106.3	8173.7	388.0	1778.0	144.7	12789.0	131.3	525.3	206.7	2821.7
5	2097.7	3393.7	3565.0	5159.0	3331.3	4867.3	5113.0	5998.7	2621.0	3657.7	1764.3	3824.3
6	3136.0	4771.3	1054.7	1456.3	5198.3	6140.3	2214.7	9811.0	4159.3	3205.0	937.3	1754.3
7	2490.3	865.3	2737.7	896.0	1584.0	4027.0	1449.3	4720.0	2674.7	2680.3	1443.0	852.7
8	3862.7	1866.7	3868.3	2635.3	5297.0	2590.3	5333.7	3706.3	3392.7	800.0	4723.7	1488.0
9	3536.7	2079.7	4816.3	1928.7	5821.7	2599.0	8793.7	3000.0	1900.3	1957.7	4503.7	1199.3
10	1214.7	627.3	516.3	888.0	2452.7	14.3	2264.3	3126.7	971.0	1730.7	1091.0	1728.0

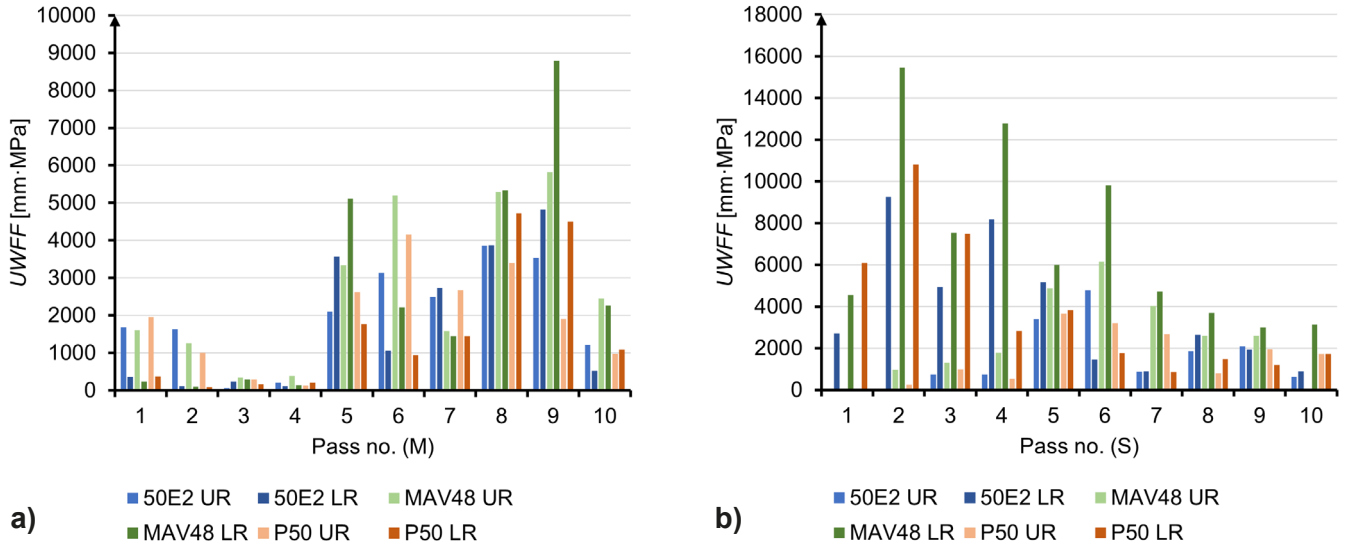

Fig. 5. Unit work of friction forces *UWFF* measured in characteristic places of subsequent passes: a) for the middle areas M, b) for the areas on the side surfaces S

greater. This trend is observed for all rails, but for the MAV48 rail, these values are the highest. In subsequent passes, the wear of the passes on the side surfaces decreases, which is related to the initial shaping of the cross-section of the rolled material. However, the wear of the passes in their central areas increases, as clearly shown by the values in Fig. 5a. Significant values of the friction force unit work are observed in pass no. 9 for the MAV48 rail, which may result from the highest total elongation coefficient ($\lambda_c = 7.05$). The greatest wear in roll pass no. 5 (the slitting cut) occurs in the central part on the cut-out knife, as shown in Fig. 4. In passes 6-10, the highest wear occurs on the surfaces shaping the rail neck, particularly the fillet radii. The rail neck elongates in these passes. Significant values of the friction force unit work are also observed during the foot shaping process, primarily in the open foot section of the cut-out. This is due to the large differences in rotational speed between the upper and lower grooves. Particular attention should be taken to pass 6 and 7 of the second stand (Fig. 6), which are coupled grooves, meaning that the middle roll constitutes the upper groove of cut 6 and the lower groove of pass 7, causing it to wear faster.

A unit friction force analysis determines the qualitative roll wear for a single rotation. A quantitative assessment of roll wear can be performed based on the roll hardness (H = 390 MPa), the wear coefficient $k_w = 3.13 \times 10^{-4}$ [12], and the length of the stock (5 m) in individual passes, calculated based on elongation coefficients. Based on this data, it is possible to calculate the number of roll rotations required to roll the appropriate length of strand after each pass. A summary of the values required to calculate roll wear is presented in TABLE 3 (where A – cross-sectional area, λ – elongation coefficient, L – length of rolled stock, ω – rotational speed).

The obtained results of numerical tests enabled the determination of the unit work of friction forces (*UWFF*), i.e. the quantitative wear of the rolls for subsequent passes (3):

$$WEAR = \frac{k_w}{HV} \cdot N \cdot UWFF \cdot \omega, \text{ mm} \tag{3}$$

TABLE 3

Rolling process parameters necessary to quantify the wear of rolls for railway rails

Pass	50E2				MAV48				P50			
	A	*λ*	*L*	*ω*	*A*	*λ*	*L*	*ω*	*A*	*λ*	*L*	*ω*
	[mm²]	[–]	[mm]	[rot/ feedstock]	[mm²]	[–]	[mm]	[rot/ feedstock]	[mm²]	[–]	[mm]	[rot/ feedstock]
feedstock	165×260 42900.0	—	5000	—	170×260 44200.0	—	5000	—	165×255 42075.0	—	5000	—
1	39784.3	1.128	5640	2.7	40823.1	1.250	6252	2.9	37299.5	1.128	5640	2.8
2	32587.3	1.203	6786	3.1	35347.3	1.203	7522	3.3	31003.6	1.203	6786	3.3
3	26047.2	1.288	8739	3.8	27324.6	1.288	9687	4.0	24073.4	1.288	8739	4.0
4	20852.7	1.229	10736	4.6	20674.7	1.229	11901	4.8	19595.7	1.229	10736	4.8
5	16180.4	1.301	13970	5.5	16207.8	1.301	15486	5.8	15058.7	1.301	13970	5.7
6	13465.5	1.223	17079	6.6	13108.2	1.223	18932	7.1	12317.8	1.223	17079	7.1
7	11296.8	1.200	20491	7.6	10781.6	1.200	22715	8.3	10266.7	1.200	20491	8.4
8	8983.4	1.213	24856	9.5	8667.8	1.213	27554	10.0	8463.6	1.213	24856	10.2
9	7148.8	1.156	28736	11.8	6983.0	1.156	31855	11.4	7320.8	1.156	28736	11.5
10	6460.0	1.097	31530	13.8	6271.8	1.097	34952	13.3	6672.1	1.097	31530	13.4

The quantitative wear of the rolls can be determined. The calculated wear values for individual roll areas are given in TABLE 4. A graphical presentation of the results is shown in Fig. 6.

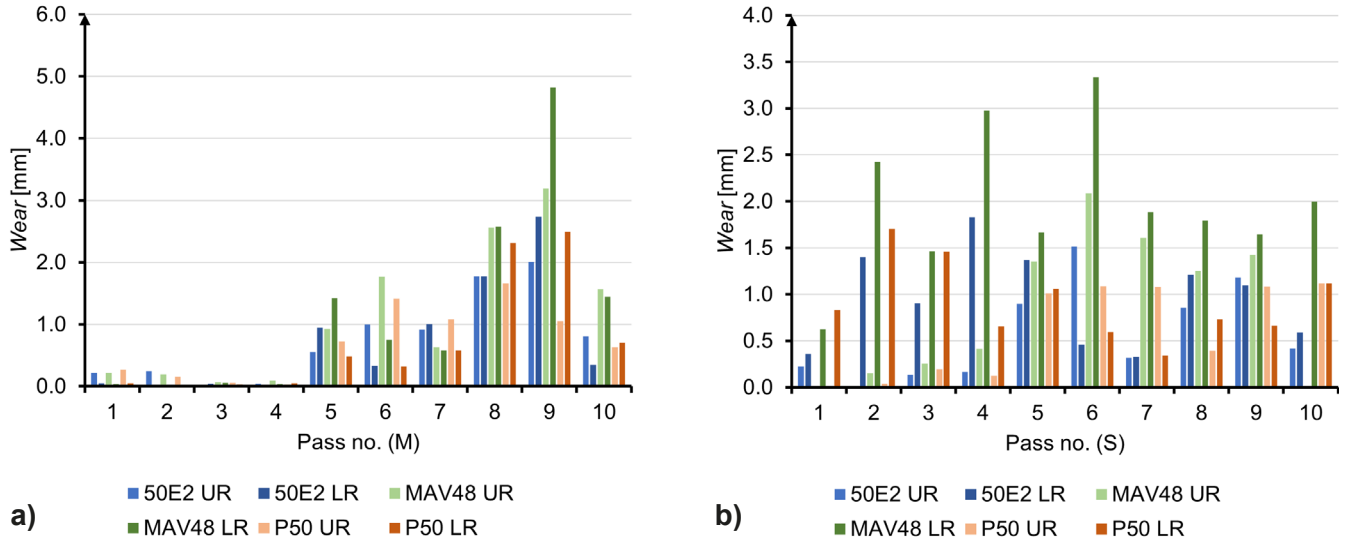

Fig. 6. Distribution of quantitative wear of the passes during the rolling of railway rails: a) for the middle areas M, b) for the areas on the side surfaces S

TABLE 4

Rolls wear values in characteristic places of the grooves

Pass no.	WEAR, [mm]											
	50E2 UR		50E2 LR		MAV48 UR		MAV48 LR		P50 UR		P50 LR	
	M	S	M	S	M	S	M	S	M	S	M	S
1	0.2	0.2	0.0	0.4	0.2	0.0	0.0	0.6	0.3	0.0	0.1	0.8
2	0.2	0.0	0.0	1.4	0.2	0.2	0.0	2.4	0.2	0.0	0.0	1.7
3	0.0	0.1	0.0	0.9	0.1	0.3	0.1	1.5	0.1	0.2	0.0	1.5
4	0.0	0.2	0.0	1.8	0.1	0.4	0.0	3.0	0.0	0.1	0.0	0.7
5	0.6	0.9	0.9	1.4	0.9	1.4	1.4	1.7	0.7	1.0	0.5	1.1
6	1.0	1.5	0.3	0.5	1.8	2.1	0.8	3.3	1.4	1.1	0.3	0.6
7	0.9	0.3	1.0	0.3	0.6	1.6	0.6	1.9	1.1	1.1	0.6	0.3
8	1.8	0.9	1.8	1.2	2.6	1.3	2.6	1.8	1.7	0.4	2.3	0.7
9	2.0	1.2	2.7	1.1	3.2	1.4	4.8	1.6	1.1	1.1	2.5	0.7
10	0.8	0.4	0.3	0.6	1.6	0.0	1.4	2.0	0.6	1.1	0.7	1.1

The data presented in Fig. 6 shows the wear of the rolls during the rolling of 50E2, MAV48, and P50 railway rails. Based on the quantitative wear of the rolls, the highest wear occurs in the final passes 8 and 9 in the central part of the rolls (primarily in the rounded areas). This is due to the relatively high deformation and elongation compared to the finishing pass. Although the rollers in pass 10 rotate a greater number of revolutions (due to elongation) to create the final rolled rail geometry, the pressing forces are not high. Therefore, the most unfavourable rolling conditions occur in passes 8 and 9, as is seen in Fig. 6a. The material in these passes also has a relatively low temperature (approximately 900°C in some areas), which causes an increase in the pressing force during forming compared to the earlier passes, where the temperature is higher. More uniform roll wear is observed in the side areas of the cuts, which affects the cut areas where the upper and lower flanges are alternately formed. The highest roll wear values were observed for the rolling of the MAV48 rail.

Based on the analysis, it can be concluded that the roll most susceptible to wear is the center roll of second stand due to the lower groove of the roll pass no. 9, for this reason, two grooves no. 9 are used on one working roll. The middle roll in second stand also experiences significant wear due to the interlocking cutouts 6 and 7, which share a common middle roll. This means that the roll in these areas will wear twice as fast as the rest of the cuts. Maintaining the required rail accuracy requires the use of four finished grooves for the last pass.

The conducted investigations of roll wear enabled the rolling of rails with improved dimensional accuracy. The analysis of roll wear, with particular emphasis on the roll pass regions most susceptible to surface degradation for the analyzed rail types, allows for a quantitative assessment of changes in roll pass geometry during operation. This issue is particularly important in the case of pre-finishing and finishing passes, which largely determine the dimensional accuracy and quality of the final product. Rails manufactured within a narrowed tolerance range are characterized by dimensional accuracy on the order of ±0.5 mm, which represents a highly demanding technological requirement for the hot rolling process.

Figure 7 shows samples taken after the rolling and straightening processes. After rolling and straightening, rails most frequently exhibit a height within the negative dimensional tolerance. This results from a reduction in height during straightening in a multi-roll straightening machine. The change in this dimension is most pronounced in rails with the thinnest web. To avoid obtaining an incorrect rail height, the rolling process is carried out in such a way that the rail height after rolling is approximately 0.5 mm greater than the nominal dimension.

4. Conclusions

The numerical analysis performed made it possible to obtain a design of the layout of passes used for rolling the selected rail shapes, with correct dimensions in accordance with the standard.

Conducted research of the railway rails rolling process allowed us to determine the wear of rolls during rolling. The developed research methodology enables the identification of characteristic intersection points where wear is the highest. The analysis indicates the areas of greatest wear of the cuts, which can be helpful in developing corrections to roll pass design and in managing rolls, their regeneration, and their operation. The assessment of the working rolls wear is one of the important economic factors when estimating the costs associated with the production of rails. Rolls and operating costs can be forecast based on the presented methodology using the finite element method during the implementation of new rails.

Funding

This work is financially supported by National Center for Research and Development (NCBiR), grant no. POIR.01.02.00-00-0173/16-00 “New railway products at Huta Królewska steel plant”.

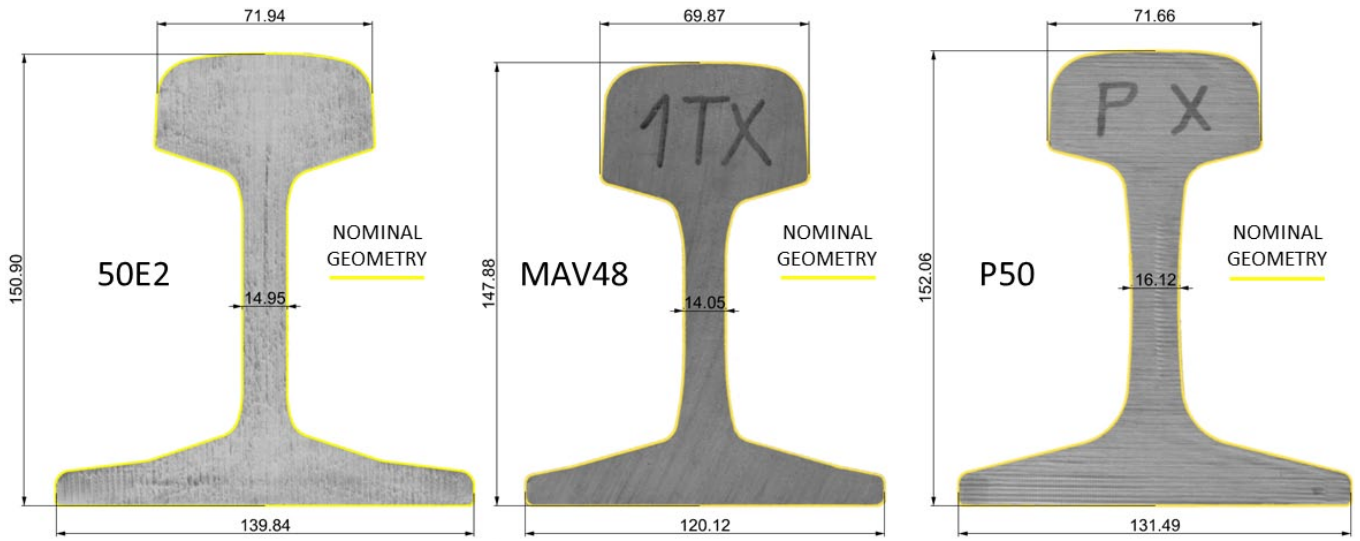

Fig. 7. Cross-sections of rolled and straightened rails

REFERENCES

[1] R. Kuziak, V. Pidvysots'kyy, M. Pernach, et al, Selection of the best phase transformation model for optimization of manufacturing processes of pearlitic steel rails. Archiv. Civ. Mech. Eng **19** (2), 535-546 (2019). DOI: https://doi.org/10.1016/j.acme.2018.12.004

[2] T. Kimura, M. Takemasa, M. Honjo, Development of SP3 rail with high wear resistance and rolling contact fatigue resistance for heavy haul railways. JFE Techn. Rep. **16**, 32-37 (2011).

[3] A. Guerrero, J. Belzunce, C. Betegon, J. Jorge, F.J. Vigil, Hot Rolling Process Simulation: Application to UIC-60 Rail Rolling. Recent Pat. Mech. Eng. **3** (1), 65-71 (2010). DOI: https://doi.org/10.2174/2212797611003010065

[4] EU-Rail. Smart and Affordable Rail Services in the EU: A Socio-economic and Environmental Study for High-Speed in 2030 and 2050; Executive Report; EU-Rail: Brussels, Belgium (2023).

[5] EN 13674-1:2011+A1:2017; Railway Applications – Track – Rail – Part 1: Vignole Railway Rails 46 kg/m and Above. BSI Standards Limited: London, UK (2017).

[6] S. Żak, D. Woźniak, The Influence of Changes in Roll Pass Design on the State of Residual Stresses in Railway Rails – Summary, Arch. Metall. Mater. **68** (2), 439-446 (2023). DOI: https://doi.org/10.24425/amm.2023.142420

[7] L. Giacomini, A. Lainati, Modern rail rolling technologies. In Proceedings of the 50 th Seminário de Laminação, Sao Paulo, Brazil, 261-273 (2013).

[8] B.M. Iljukovich, N.E. Nekhajev, S.E. Merkurev, Prokatka i Kalibrovka (Rolling and Roll Pass Design); RVA Dnipro-VAL: Dnipropietrovsk, Ukraine, (2002).

[9] E. Wosiek, A. Nowakowski, Kalibrowanie Walców (Roll Pass Design), 3rd ed.; Academy of Mining and Metallurgy: Kraków, Poland, (1981).

[10] V. Danchenko, H. Dyja, L. Lesik, L. Mashkin, A. Milenin, Technologia i Modelowanie Procesów Walcowania w Wykrojach (Technology and Modelling of Rolling Processes in Shapes); WIPMiFS: Czestochowa, Poland, (2002).

[11] S. Spuzic, K.N. Strafford, C. Subramanian, G. Savage Wear of hot rolling mill rolls: An overview. Wear **176**, 261-271 (1994).

[12] P. Szota, S. Mróz, A. Stefanik, T. Zygmunt, M. Bołda, Analysis of Roll Pass Wear in the Railway Rail Rolling Process. Materials **18**, (2025). DOI: https://doi.org/10.3390/ma18225131

[13] A. Karmakar, S. Sethuramiah, A. Wear of Materials **2**, ASME, New, York, NY, USA, (1991).

[14] F. Lambiase, A. Langella, Antonio. Automated Procedure for Roll Pass Design. Journal of Materials Engineering and Performance **18**, 263-272 (2009). DOI: https://doi.org/10.1007/s11665-008-9289-2

[15] H.-C. Kwon, Y.-T. Im, Interactive computer-aided-design system for roll pass and profile design in bar rolling. J. Mater. Process. Technol. **123** (3), 399-405 (2002). DOI: https://doi.org/10.1016/S0924-0136(02)00100-0

[16] B. Huang, K. Xing, K. Huang, H. Lan, Development of a geometric modelling strategy for roll pass optimal design. Rob. Comput. Integr. Manuf. **30**, 622-628 (2014). DOI: https://doi.org/10.1016/j.rcim.2014.04.006

[17] EN 13674-4 is the European standard for railway rails.

[18] GOST R 51685-2022 is the Russian technical standard for railway rails.

[19] EN 13674-1 is the European standard for railway rails.

[20] S. Mróz, P. Szota, A. Stefanik, H. Dyja, Microstructure Numerical Modelling Change during the Round Bars Rolling. Mater. Sci. Forum **715-716**, 883-888 (2012). DOI https://doi.org/10.4028/www.scientific.net/msf.715-716.883

[21] https://www.transvalor.com/en/forge (accessed on 01.12.2025)

[22] F.H. Norton., Creep of steel at high temperature, McGraw Hill, New York, USA, (1929).

[23] N.J. Hoff, Approximate analysis of structures in the presence of moderately large steps deformation. Q. Appl. Math. **12**, (1) 49-55 (1954).

[24] A. Hansel, T. Spittel, Kraft und Arbeitsbedarf Bildsomer Formgeburgs Verfahren, VEB Deutscher Verlang fur Grundstoffindustrie, Lipsk, Germany, (1979).

[25] J.F. Archard, Contact and Rubbing of Flat Surfaces. J. Appl. Phys. **24**, 981-988 (1953). DOI: https://doi.org/10.1063/1.1721448